

CHIMERA LIQUID SOLID HYBRID ROCKET

SOFTWARE TEAM LEAD: CAMERON PELKEY

CONTRIBUTORS: CHRIS KONG AND JACOB VERMEER

NOVEMBER 3RD, 2023

HADES Engine Software Model

Contents

- 0.1 Purpose: 2
 - 0.1.1 The Code Flow: 2
- 0.2 The Model: 3
 - 0.2.1 Blowdown Oxidizer Tank Model: 3
 - 0.2.2 Combustion Chamber Model: 4
 - 0.2.3 Nozzle and Exit Velocity Model: 7
 - 0.2.4 Termination Events: 8
- 0.3 Inputs: Nov 8th 9
- 0.4 Outputs: Nov 8th 10
- 0.5 Conclusion: 13
 - 0.5.1 Room for Improvement - Refining the Model for the Future: 13
- 0.6 Appendix: 14
 - 0.6.1 Appendix.A: Oxidizer Tank Pressure 14
 - 0.6.2 Appendix.B: Chamber Pressure 15
 - 0.6.3 Appendix.C: Injector Flow Models 16
 - 0.6.4 Appendix.D: Derivations of Thrust and Exit Velocity 18
 - 0.6.5 Appendix.E: Disk Filter 19
- 0.7 Works Cited: 20

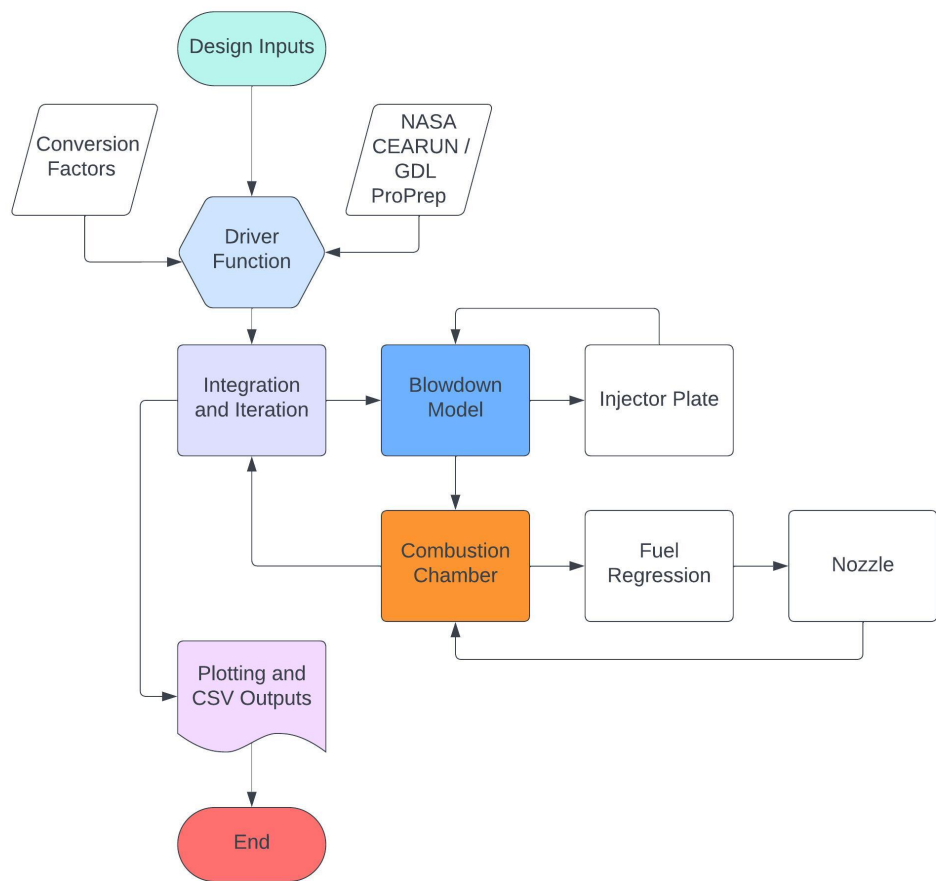
0.1 Purpose:

Based on Rhode’s First Principle model, we hoped to develop a model with higher creative freedom to start designing the liquid-solid hybrid rocket engine HADES. The reason why we need a higher fidelity and credibility of the software model is due to the need to predict the thrust of the rocket we build accurately. Here are the requirements pertaining to this software model.

Requirements	Verification
FR. 1 All designs, tests, and operations shall pose no safety risk to any persons, property, or environment.	The resulting simulation shall meet all required factors of safety
FR . 7 The vehicle shall maintain structural integrity during flight.	The resulting simulation shall not exceed structural limitations
FR. 8 Theoretical modeling shall be completed and performance predicted prior to flight	The resulting simulation has measurable outputs of thrust and impulse
FR. 9 The vehicle shall achieve liftoff.	The resulting simulation has thrust and impulse greater than system weight

Table 1: Requirements

0.1.1 The Code Flow:



The image above outlines the current high-level tasks the software code undergoes. The heart of the equations we will discuss is found in the integration and iteration loop. Here, the inputs and outputs are fed into each other over time until termination events occur. The most common, and should be the most common, termination event is when fuel runs out. After this, all of the outputs will be plotted and fed into CSV files.

0.2 The Model:

Leaving Rhode's First Principles, we moved forward with the first principles such as Bernoulli's Compressible flow and the ideal gas law while incorporating new models throughout the stages of the rocket.

0.2.1 Blowdown Oxidizer Tank Model:

The governing equations for the blowdown model include ...

1. Ideal Gas Law
2. Conservation of Mass
3. Bernoulli's Compressible Flow

The assumptions for the blowdown model include...

- Single Phase injector
- Pressure of the entire tank is determined by the ullage gas
- Constant temperature (walls of the tank are adiabatic)
- Liquid Nitrous Oxide is only in the liquid state and acts as an incompressible liquid
- The Ullage gas will act as an Ideal Gas
- There is no leakage, all mass flow goes into the drain port

The important equations include

$$\dot{m}_{ox} = C_{d_{inj}} \cdot A_{inj} \cdot \sqrt{2 \cdot \rho_{ox} \cdot (P_{tank} - P_{chmb})} \quad (1)$$

This equation calculates the oxidizer mass flow for a single-phase injector. One thing to note is that in the code, from the perspective of the combustion chamber, this is a positive value. However, from a holistic view, this should be negative as it is being expelled from the engine.

$$\frac{\partial V_u}{\partial t} = - \left(\frac{\partial V_{ox}}{\partial t} \right) = \frac{-\dot{m}_{ox}}{\rho_{ox}} \quad (2)$$

This equation calculates the change in volume of the ullage gas with respect to time and is used to find V_u at any time step.

$$\frac{\partial P_{tank}}{\partial t} = \frac{P_{u_i} \cdot V_{u_i}}{(V_u)^2} \cdot C_D \cdot A_{inj} \sqrt{\frac{2}{\rho_{ox}} (P_{ox} - P_{chmb})} \quad (3)$$

This equation calculates the change in oxidizer tank pressure with respect to time. For more information, please look at the appendix Appendix.A.

0.2.2 Combustion Chamber Model:

The governing equations for the combustion chamber model include ...

1. Conservation of Mass
2. Ideal Gas Law

The assumptions for the combustion chamber model include ...

- Combustion chamber is adiabatic, there is no heat loss to the environment
- Choked Flow of Nozzle inlet
- Flow through the combustion chamber is uniform and non-rotational
- Complete combustion of oxidizer and fuel, only gaseous products contribute to the pressure change
- Combustion is uniform across the fuel grain
- Fuel grain burnings occur normal to the axial direction in a uniform matter
- Pressure is uniform across the entire combustion chamber
- Temperature is uniform across the entire combustion chamber

Fuel Regression Model:

The fuel regression model to be used is called the Marxmann and Gilberts Law. It is the following...

$$\dot{r} = a \cdot G_{ox}^n \quad (4)$$

Where

- \dot{r} is the burn rate in *in/s* or *mm/s*
- a is a property of the fuel for its burn coefficient
- G_{ox} is the mass flux of the liquid oxidizer. This can also be viewed as

$$G_{ox} = \frac{\dot{m}_{ox}}{A_{port}} \quad (5)$$

where the A_{port} is the combustion port cross-sectional area.

One thing to note is the following:

$$ConversionFactor = (0.0254^{(1+2n)}) \cdot (0.453592^n) \quad (6)$$

Based on n value which is always less than 1, this conversion factor is necessary to correct a to have the correct units.

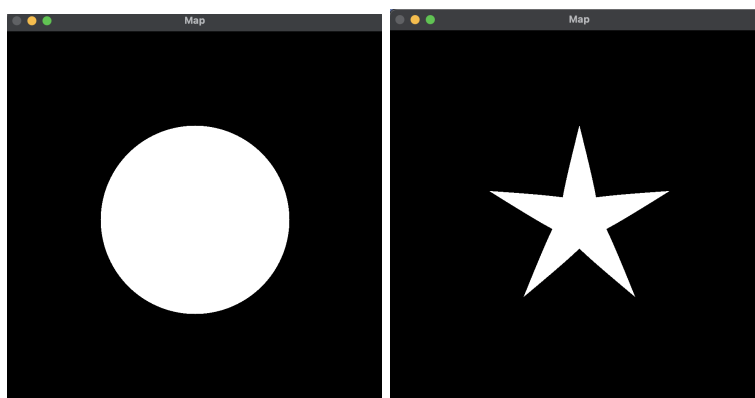
Burn Back Tables

To further increase the credibility of the fuel regression models and add the creative freedom to have complex fuel geometries, we have investigated the industry standards of what is called a Burn Back Table. This increases the complexity of the software model, however, the product should improve the fidelity of the fuel regression while simultaneously allowing the iteration of complex fuel geometries to focus on the thrust values, chamber properties, and fuel mass flow we want.

To build the burn back tables, there are three key components: the initial fuel geometry, the disk filter applied, and the contours shaped from each iteration. Let us break down those critical components.

1) Initial Fuel Geometry

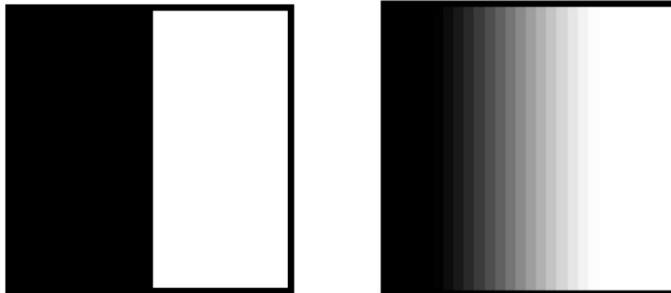
Using Python open cv (An open-source computer vision library), we are able to create pixelated cross-section areas of a given fuel grain. However, defining and determining how to build each geometry is complex and quite difficult. Luckily, to create this model Open Motor (An open-source solid rocketry library) has Python code to start creating their geometries. Using these we can have a starting point on a variety of complex fuel geometries such as star, wagon wheel, and spoke wheel. Here are some of the initial geometries we explored...



The initial geometry allows us to apply the disk filter and contour lines. Thus it is such an important step. After a given fuel geometry, we have developed the code such that it is plug and play into the rest of the analysis to developed the fuel regression. An example is shown below as a basic example.

2) Disk Filter

The choice to have the pixelated image be black and white is intentional. It eases into the use of a disk filter, or blur, on the image to simulate the fuel burning.



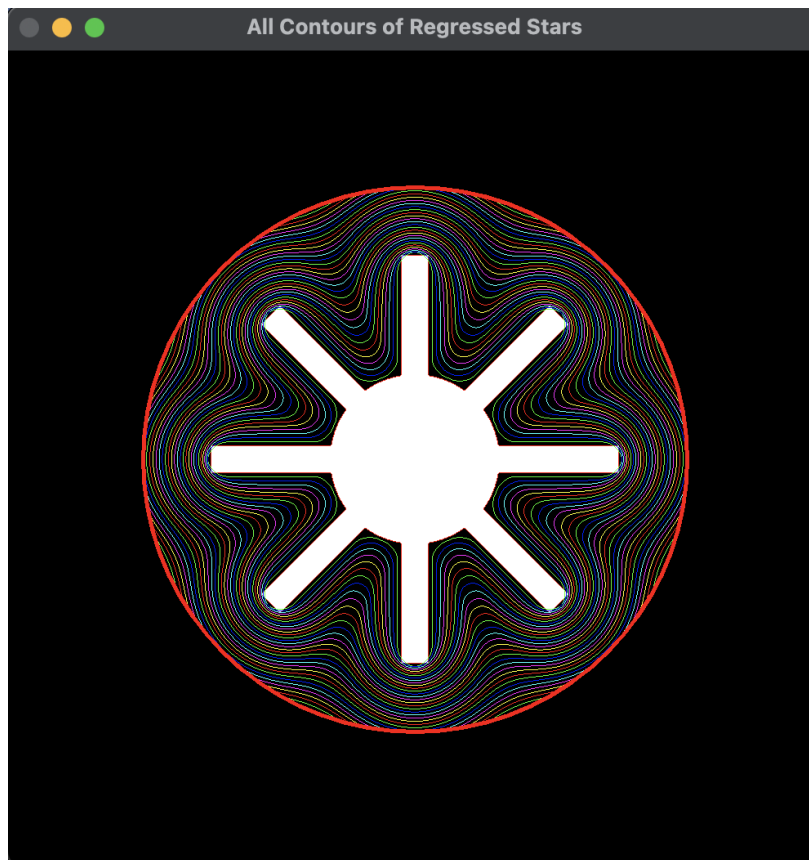
The image on the left represents a normal fuel (black) and the open propellant gas volume (white). Once a disk filter is applied, it blurs the image to have a grey scale in between the absolute black (0) and absolute white (255). Applying this disk filter blur can replicate the effect of combustion, transient heat effects, and essentially how the fuel will likely burn.

Another important aspect is applying a pixel threshold. The key question is, how much of the gray pixels burns and does it reflect what happens during a real burn? This is another unknown that unfortunately will not be known until a static fire. However, given the iterative nature of software we are able to scope out margins of that error.

For more information, disk filter will be outlined in Appendix. E.

3) Contour Lines

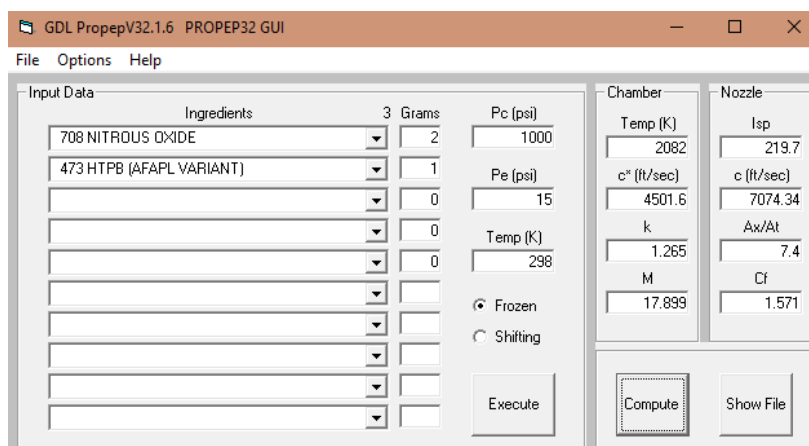
That last and most important part of creating the black and white images is finding the contour line that demarcates and separates the black and white pixels. Using open cv intrinsic liked findCountour() does this easily with little to no error. Then calculating perimeter and area can aid us in the calculation of a complex fuel geometries A_{port} , A_b and V_{chmb} .



Then after each iteration, the contour lines and related calculations can be stored and called depending on the calculated fuel regression \dot{r} . Furthermore, interpolation and fitting of the burn back table can be calculated for values in between indexed \dot{r} .

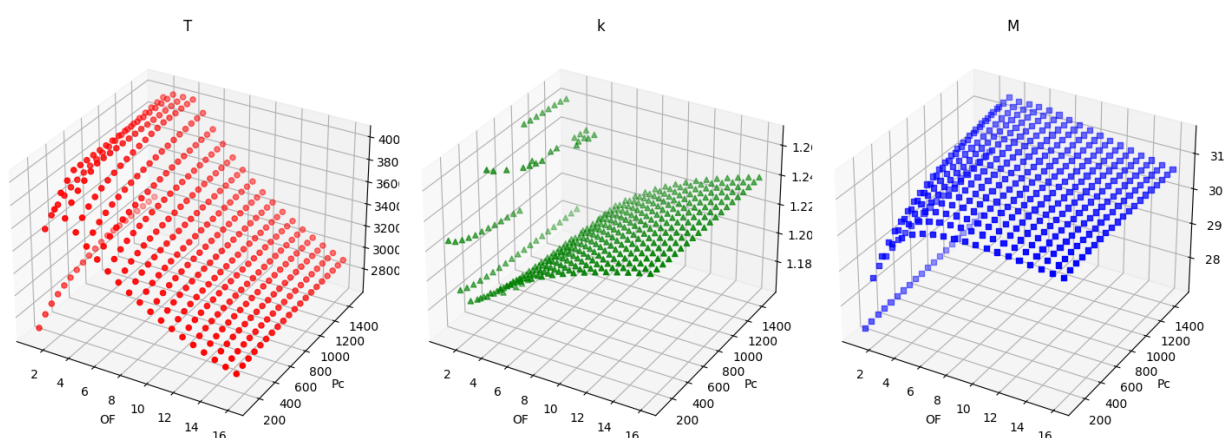
GDL Proprep Implementation:

The previous models consider the parameters inside the combustion chamber, like temperature and molecular weight, to be constant. This is not true as the oxidizer-to-fuel ratio changes as the rocket propels. Thus multiple things are necessary to create this. First, let's look a GDL Proprep and how our inputs affect the outputs.



As we can see with this simple screen capture, a mixture of Nitrous Oxide with HTPB with an OF ratio of 2 results in knowing the chemical properties inside the combustion chamber. Therefore, we can exploit this by running an iterative macro to change the OF ratio and chamber pressure.

Over a varying range of OF ratios from 1 to 14 and a varying chamber pressure (P_c) from 100 to 1500 psi the following graphs were created.



From these graphs we are able to have a lookup table that can be incorporated into the iterative process to update the necessary chamber properties such as chamber temperature, the ratio of specific heats (γ or in GDL k), and the molecular weight. As we increase the precision of the oxidizer-to-fuel ratio and chamber pressure, the fidelity of the model will increase.

Combustion Model:

The important equations include

$$A_{port} = \pi \cdot r^2 \quad (7)$$

This equation calculates the combustion port cross-sectional area at a time step based on the radius of the fuel grain r .

$$A_b = 2 * \pi * r * L \quad (8)$$

This equation calculates the current burnable surface area of the fuel grain at a time step based on the radius of the fuel grain r .

$$V_{chmb} = \pi \cdot r^2 \cdot L \quad (9)$$

This equation calculates the current gaseous volume of the chamber at a time step based on the radius of the fuel grain r .

$$\rho_{chmb} = \frac{P_{chmb}}{R' \cdot T_{chmb}} \quad (10)$$

This equation calculates the current gaseous density of the chamber at a time step. This is a form of $PV = nRT$ or the Ideal gas law.

$$R' = R_u / M \quad (11)$$

This equation calculates the R' gas constant of the combustion chamber gas that is created. This is found from inputs from GDL ProPrep or NASA CEARUN.

$$\dot{m}_f = \rho_f \cdot A_b \cdot \dot{r} \quad (12)$$

This equation calculates the mass flow of the fuel grain at a time step based on the radius of the fuel grain.

$$\frac{\partial P_{chmb}}{\partial t} = \frac{R' \cdot T_{chmb}}{V_{chmb}} \cdot \left[A_b \dot{r} (\rho_f - \rho_{chmb}) + \dot{m}_{ox} - P_{chmb} \cdot A_t \sqrt{\frac{\gamma}{R' T_{chmb}}} \left(\frac{2}{\gamma + 1} \right)^{\left(\frac{\gamma + 1}{2(\gamma - 1)} \right)} \right] \quad (13)$$

This equation calculates the change in combustion chamber pressure with respect to time.

0.2.3 Nozzle and Exit Velocity Model:

The governing equations for the nozzle model include ...

1. Newton's Second Law $F = ma$ (or $F = \dot{m}v$)
2. Continuity Equation for Compressible Flow $\rho_1 A_1 v_1 = \rho_2 A_2 v_2$
3. Isentropic Flow Relationships

$$\frac{P_0}{P} = \left(1 + \frac{\gamma - 1}{2} M^2\right)^{\frac{\gamma}{\gamma - 1}} \quad (14)$$

The assumptions for the nozzle model include ...

- Combustion gases can be treated as calorically perfect gases
- One-dimensional, Isentropic, Inviscid, Compressible Flow
- Nozzle Throat diameter undergoes no regression / deterioration in operation
- Nozzle exit pressure is approximately equal to ambient pressure for the duration of engine operation

The important equations include ...

$$\left(\frac{A}{A^*}\right)^2 = \frac{1}{M^2} \left[\frac{2}{\gamma - 1} \left(1 + \frac{\gamma - 1}{2} M^2\right) \right]^{\frac{\gamma + 1}{\gamma - 1}} \quad (15)$$

This equation is the primary driver of our nozzle design. It allows us to calculate our ideal expansion ratio for the nozzle given the desired exit mach number. We design for ideal expansion, so this exit mach number is purely a function of chamber pressure and ambient pressure, and is calculated by root-solving equation 14 for

$$\frac{P_0}{P} = \frac{P_0}{P_{exit}} = \frac{P_0}{P_{ambient}}$$

Which is known as the "design condition" for the nozzle. Given M_e , equation 15 allows us to calculate the necessary area ratio $\frac{A_e}{A^*} = \frac{A_e}{A_t}$ for perfect expansion of our nozzle. The combustion chamber model gives us our design A_t , so multiplying

$$\frac{A_e}{A_t} \cdot A_t = A_e$$

Gives us the nozzle exit area necessary for perfect expansion.

$$F = A_t \cdot P_{chmb} \sqrt{\left(\frac{2\gamma^2}{\gamma - 1}\right) \left(\frac{2}{\gamma + 1}\right)^{\frac{\gamma + 1}{\gamma - 1}} \left[1 - \left(\frac{P_e}{P_{chmb}}\right)^{\frac{\gamma - 1}{\gamma}}\right]} \quad (16)$$

This equation calculates the force of thrust created by the engine as a function of chamber pressure (and γ , the ratio of specific heats). It is derived from the continuity equation for compressible flow, evaluated at the choked throat of the nozzle. This continuity equation establishes the mass flow rate of combustion products through the nozzle, which is then multiplied by the exit velocity per Newton's Second Law to obtain the total thrust.

An in-depth derivation of this exit velocity equation can be found in Appendix D. It is important to note that the exit velocity equation relies on the assumption that the flow through the nozzle is entirely isentropic. In reality, during the majority of the engine operation oblique shocks will form at the exit of the nozzle which will cause large jumps in the enthalpy of the flow, breaking this isentropic assumption. Thus, the thrust model provided by equation 16 provides an idealized thrust output and potentially warrants improvements via incorporating the effect of these oblique shocks.

Another potential improvement to this nozzle model is the inclusion of a constant factor to account for the three-dimensional expansion of the flow. Our model is derived based on a two-dimensional cross section of the nozzle, which is approximately correct but obviously nonphysical. One method is provided by Sutton, and this will be researched soon.

0.2.4 Termination Events:

For a realistic simulation of the engine, there must be checks at every time step that logically reflect what will happen. If these checks were to be met, it is safe to assume that the model has done its job and is okay to stop.

- Mass of the Liquid Nitrous Oxide is equal to zero
- Mass of the Fuel Grain is equal to zero
- Radius of the Port is equal to the fuel grain's outer diameter
- Pressure of the combustion chamber is greater than or equal to the pressure inside the oxidizer tank

Reasoning:

Each termination event is implemented into the code for a reason. They are motivated because without them the model will run indefinitely

- If the mass of the liquid nitrous oxide is equal to zero, that means that there is no more nitrous oxide in the oxidizer tank. This means that the assumptions of the combustion reaction are invalid as one of the primary reactants in the combustion reaction is missing.
- If the mass of the fuel grain is equal to zero, that means that there is no more fuel grain in the combustion chamber. This means that the assumptions of the combustion reaction are invalid as one of the primary reactants in the combustion reaction is missing.
- If the radius of the port is equal to the fuel grain's outer diameter, that means there is no more fuel left to burn. This means that the assumptions of the combustion reaction are invalid as one of the primary reactants in the combustion reaction is missing.
- If the pressure of the combustion chamber exceeds the pressure inside the oxidizer tank, that means the high-temperature combustion gas may experience back flow into the oxidizer tank rather than flow toward the nozzle. This is something the model does not simulate as this will lead to a failure for the rocket.

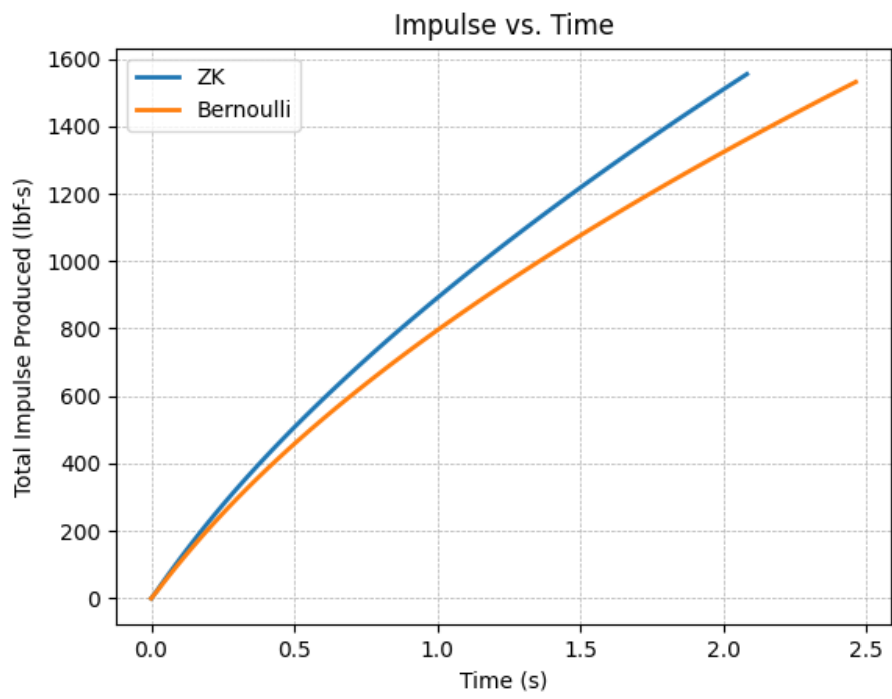
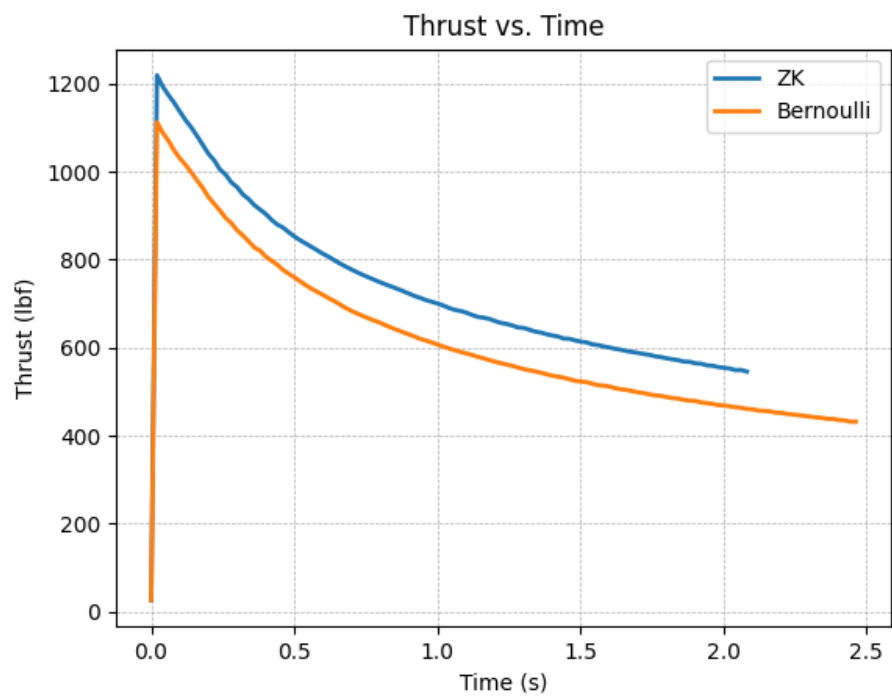
0.3 Inputs: Nov 8th

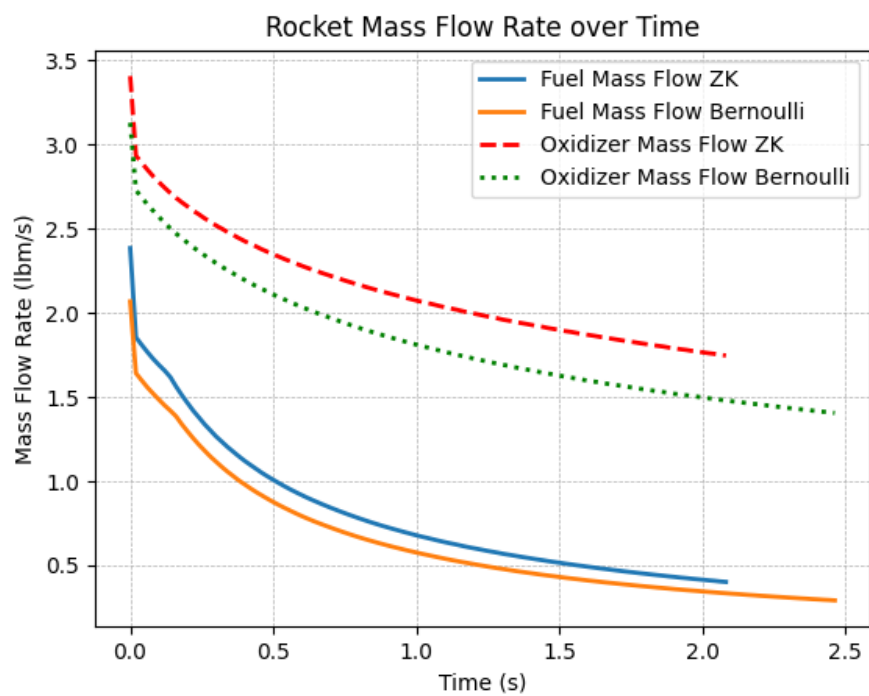
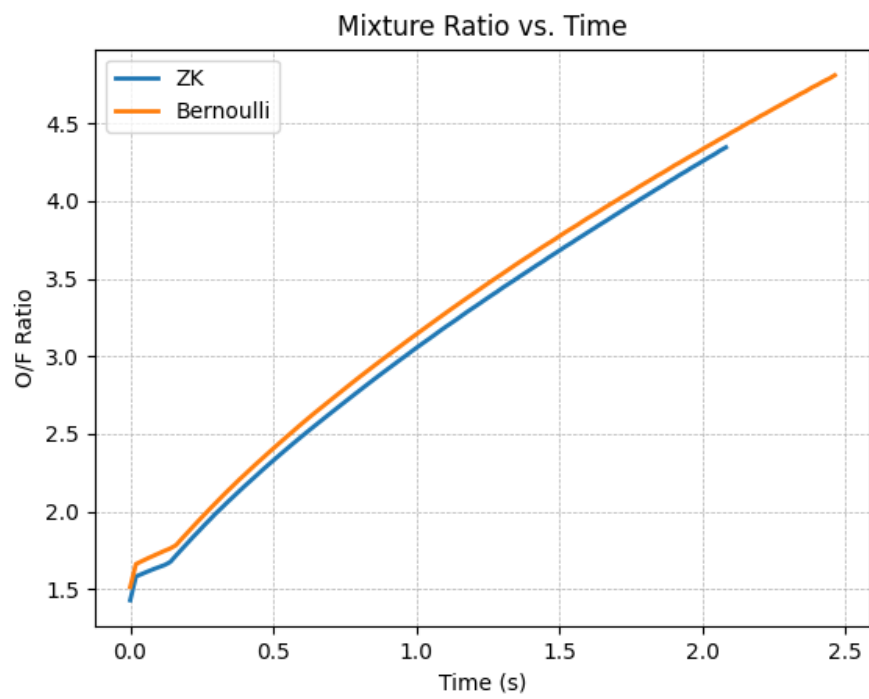
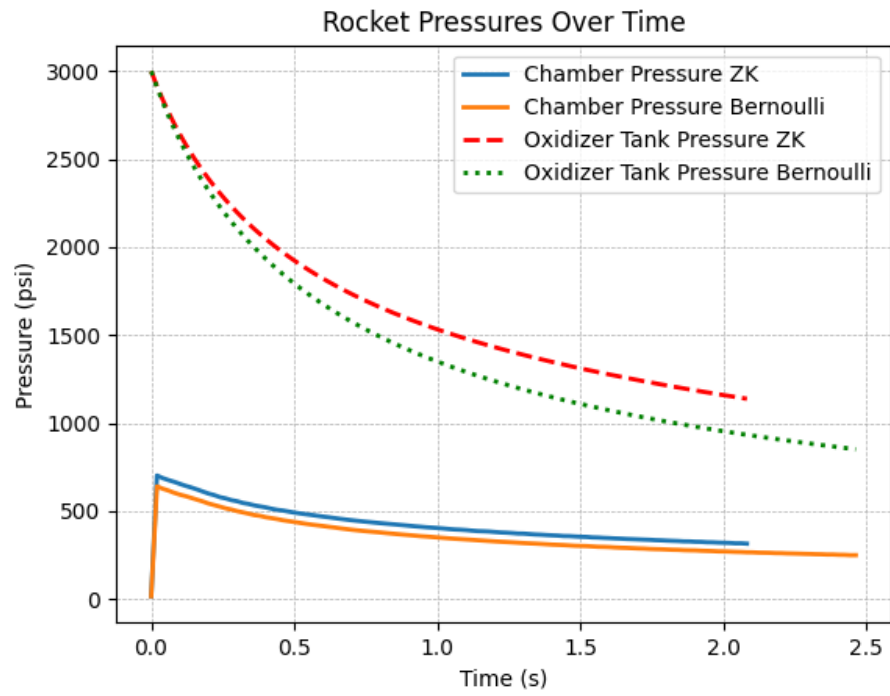
This section tabulates the inputs to the model. The base model is built on ballpark estimates and are tabulated below.

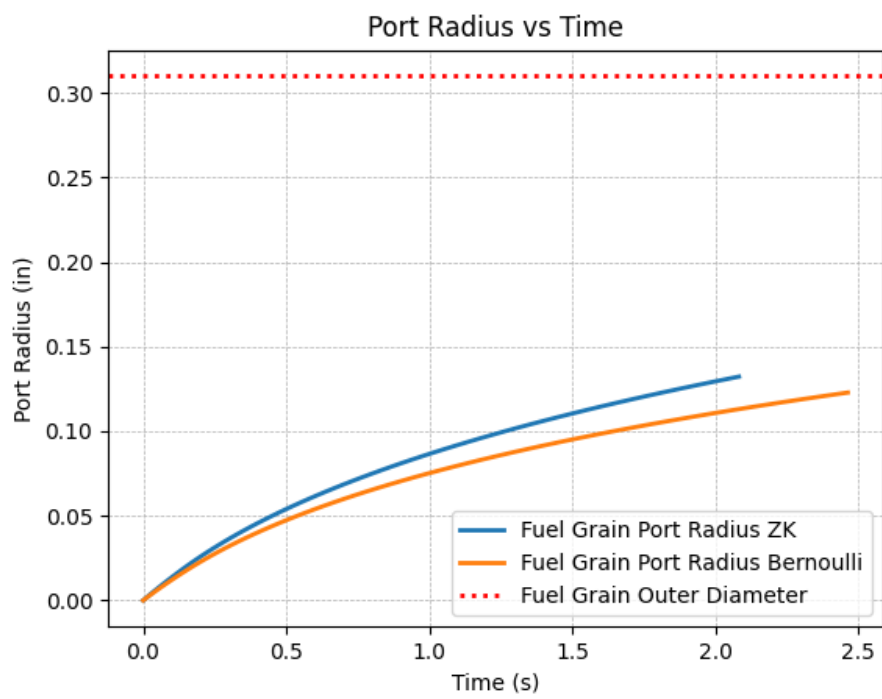
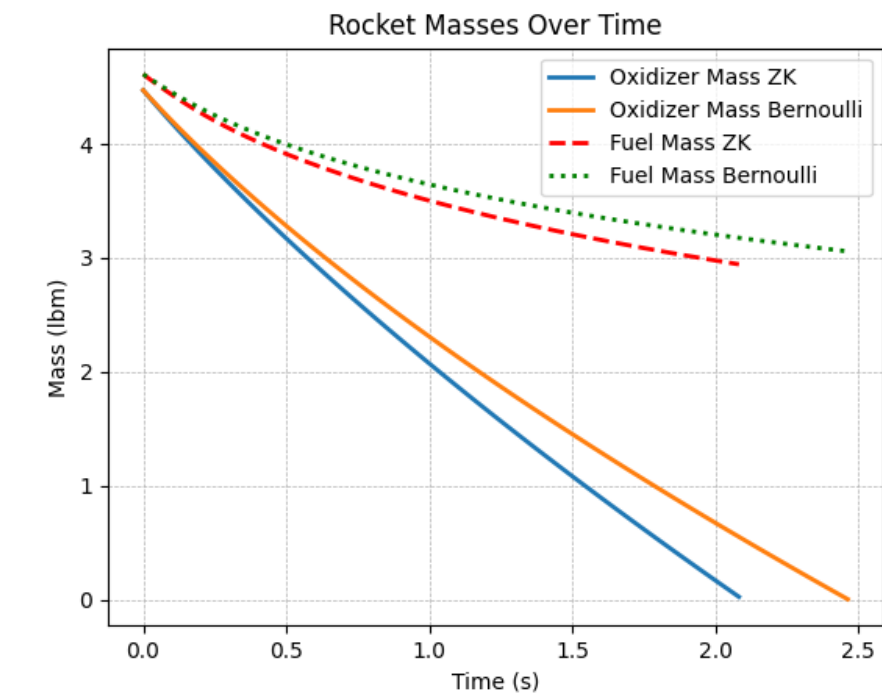
MODEL	VARIABLE	DESCRIPTION	UNITS	VALUE
Ambient	-	-	-	-
	P_{amb}	Ambient Pressure	[Pa]	$1.026e + 5$
	T_0	Ambient Temperature	[K]	288
	R_u	Universal Gas Constant	$[J/(mol * K)]$	8.3145
Blowdown	-	-	-	-
	V_{tank}	Oxidizer Tank Volume	$[m^3]$	0.003
	P_{tank}	Initial Oxidizer Tank Pressure	[Pa]	$2.068e + 7$
	M_{N2O}	Initial Oxidizer Mass	$[kg]$	2.1
	M_{Tank}	Mass of Oxidizer Tank	$[kg]$	2.1
	ρ_{ox}	Liquid Nitrous Oxide Density	$[kg/m^3]$	1226
	A_{inj}	Area of Injector	$[m^2]$	$9.4e - 6$
	$C_{D_{inj}}$	Coefficient of Discharge of Injector	[-]	0.4
Combustion Chamber	-	-	-	-
	$Fuel_{OD}$	Fuel Grain Outer Diameter	[m]	0.0343
	L	Length of Fuel Grain	[m]	0.3048
Fuel Regression	-	-	-	-
	a	Burn Rate Coefficient	[-]	$9.33e - 08$
	n	Burn Rate Coefficient	[-]	1.681
	ρ_{fuel}	Fuel Grain Density	$[kg/m^3]$	2089.83
Nozzle	-	-	-	-
	D_t	Diameter of Nozzle Throat	$[m^2]$	0.03048
	α	Nozzle Diverging Half-Cone Angle	[rad]	0.2618

Table 2: Input Data for Each Part of the Model - Metric

0.4 Outputs: Nov 8th

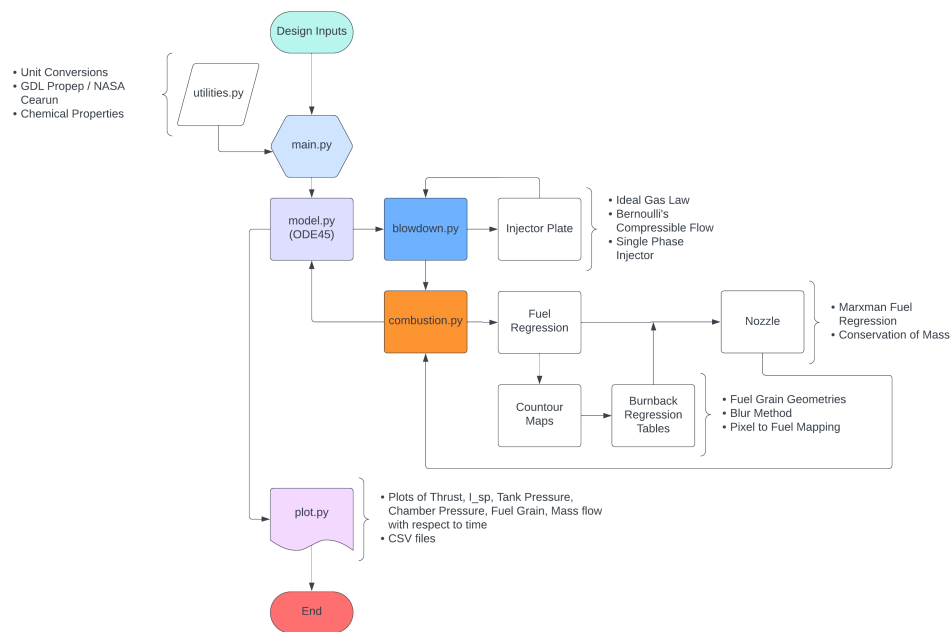






0.5 Conclusion:

The following code follows a flow chart like this. There are more specifics in this flow chart rather than the higher level one.



0.5.1 Room for Improvement - Refining the Model for the Future:

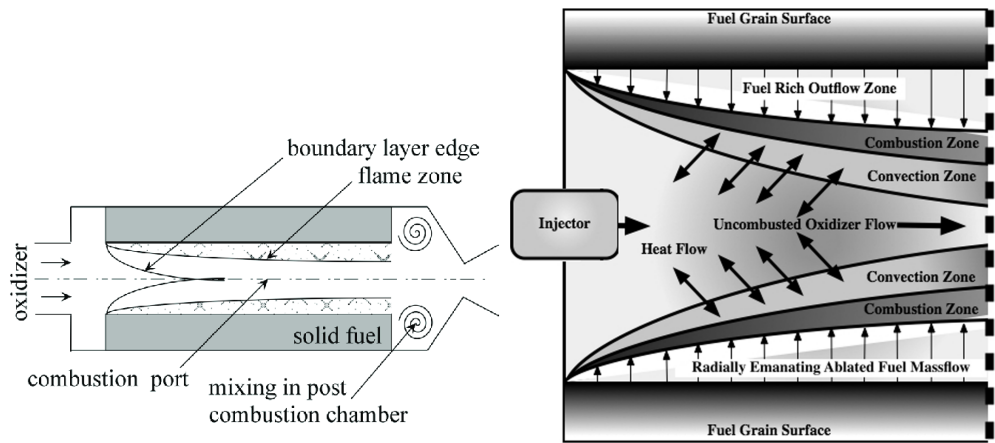
Here are some possible leads that can be investigated further for implementing the model. There is room for improvement but it is a trade on man-hours versus uncertainty with calculations.

Blowdown Model

- Consider the effect of not just gaseous ullage and liquid nitrous oxide but the vaporous nitrous oxide that might occur in phase equilibrium, models may include the Peng-Robinson equation of state or the Zilliac-Karaberough Model.

Combustion Chamber Model

- In the pressure chamber, there are three states of pressure. Start-up, Steady-state, and Tail-off. In this model, a steady state was implemented. Start-up and Tail-off implementations may improve the model
- For fuel regression, there is a conical shape that follows the propellant burning in a axial motion. This can greatly effect the change of mass flow throughout the chamber as more burnable surface area shows itself rather than the uniform burn assumption. A image is as follows...



0.6 Appendix:

0.6.1 Appendix.A: Oxidizer Tank Pressure

Starting with the Ideal Gas Law, we can see the following.

$$P_{u_i} \cdot V_{u_i} = n \cdot R_u \cdot T_{tank} \quad (17)$$

The initial pressure and volume of the ullage gas can be found with the number of moles (n), universal gas constant, and the temperature of the tank. Furthermore, assumptions such as the pressure of the ullage is equivalent to the pressure of the oxidizer tank means that $P_u = P_{tank}$. This is further backed up as the liquid nitrous oxide acts as an incompressible fluid.

$$P_{u_i} \cdot V_{u_i} = P_u \cdot V_u \quad (18)$$

The temperature of the oxidizer tank decreases over time as the liquid nitrous leaves the tank and the ullage gas expands. However, due to the length of the rocket burn, the temperature change is negligible. Therefore, the assumption is that the tank is at a constant temperature and the control volume is adiabatic with respect to the tank walls. The entire system can be seen to have constant temperature. This allows us to use Boyle's Law such that $P_1 V_1 = P_2 V_2$.

Solving the equation such that the pressure can be defined by any volume state at any time, differentiating the equation allows us to find the change in oxidizer tank pressure with the change in ullage gas volume.

$$\begin{aligned} P(V_u) &= \frac{P_{u_i} \cdot V_{u_i}}{V_u(t)} \\ \frac{\partial P_{ox}}{\partial V_u} &= \frac{\partial}{\partial t} \left(\frac{1}{V_u(t)} \right) \cdot P_{u_i} \cdot V_{u_i} \\ \frac{\partial P_{ox}}{\partial V_u} &= \frac{-P_{u_i} \cdot V_{u_i}}{(V_u(t))^2} \end{aligned}$$

The last differential equation to find is the change in volume with respect to the change in time. This is found using Bernoulli's compressible flow equation. There are two versions of the equation and both work. To go in between the two flow rate equations just multiply by density such as $m = \rho \cdot V$.

$$\begin{aligned} Q &= \frac{\partial V_{ox}}{\partial t} = C_D \cdot A_{inj} \sqrt{\frac{2}{\rho_{ox}} (P_{ox} - P_{chmb})} \\ \dot{m}_{ox} &= \frac{\partial m_{ox}}{\partial t} = C_D \cdot A_{inj} \sqrt{2 \cdot \rho_{ox} (P_{ox} - P_{chmb})} \end{aligned}$$

The first equation is the volumetric flow rate of the liquid nitrous oxide across the injector while the second equation is the mass flow rate of the liquid nitrous oxide across the injector. Through some manipulation. We can see that the volume flow of the liquid oxidizer will be equal to the volume gain of the ullage gas.

$$\frac{\partial V_u}{\partial t} = - \left(\frac{\partial V_{ox}}{\partial t} \right) = -C_D \cdot A_{inj} \sqrt{\frac{2}{\rho_{ox}} (P_{ox} - P_{chmb})} \quad (19)$$

Now with the two differential equations, we can solve the chain rule for the change in oxidizer tank pressure with respect to time.

$$\begin{aligned} \frac{\partial P_{ox}}{\partial t} &= \frac{\partial P_{ox}}{\partial V_u} \cdot \frac{\partial V_u}{\partial t} \\ \frac{\partial P_{ox}}{\partial t} &= \frac{-P_{u_i} \cdot V_{u_i}}{(V_u(t))^2} \cdot -C_D \cdot A_{inj} \sqrt{\frac{2}{\rho_{ox}} (P_{ox} - P_{chmb})} \\ &= \frac{P_{u_i} \cdot V_{u_i}}{(V_u)^2} \cdot C_D \cdot A_{inj} \sqrt{\frac{2}{\rho_{ox}} (P_{ox} - P_{chmb})} \end{aligned}$$

0.6.2 Appendix.B: Chamber Pressure

Starting with the conservation of mass. It is evident that all of the mass that enters and exits throughout the combustion chamber must be equal. Another way to view this is the rate of combustion product generation is equal to the rate of consumption of the propellant grain. Therefore, we can simplify the mass flow into four main parts

$$\dot{m}_g + \dot{m}_{ox} = \frac{\partial M_s}{\partial t} + \dot{m}_{noz} \quad (20)$$

What enters the system, the left-hand side is the mass flow generated due to the burning fuel from the fuel regression model and the mass of the oxidizer that comes from Bernoulli's compressible flow from the blowdown model. What exits the system, on the right-hand side is the mass due to the change in gas volume from propellant consumption and the mass flow through the nozzle.

We can expand each of these four mass flows into their respective parts as follows.

$$\begin{aligned} \dot{m}_g &= A_b \cdot \rho_f \cdot \dot{r} \\ \dot{m}_{ox} &= C_D \cdot A_{inj} \sqrt{2 \cdot \rho_{ox} (P_{ox} - P_{chmb})} \\ \frac{\partial M_s}{\partial t} &= A_b \cdot \rho_{chmb} \cdot \dot{r} + V_{chmb} \frac{\partial \rho_{chmb}}{\partial t} \\ \dot{m}_{noz} &= P_{chmb} \cdot A_t \sqrt{\frac{\gamma}{R' T_{chmb}}} \left(\frac{2}{\gamma + 1} \right)^{\left(\frac{\gamma+1}{2(\gamma-1)} \right)} \end{aligned}$$

Now we can substitute these into the conservation of mass with the addition of the fuel regression model. One thing to note is that \dot{m}_{ox} will not be substituted because it is in its most simplified form.

$$A_b \cdot \rho_f \cdot \dot{r} + \dot{m}_{ox} = A_b \cdot \rho_{chmb} \cdot \dot{r} + V_{chmb} \frac{\partial \rho_{chmb}}{\partial t} + P_{chmb} \cdot A_t \sqrt{\frac{\gamma}{R' T_{chmb}}} \left(\frac{2}{\gamma + 1} \right)^{\left(\frac{\gamma+1}{2(\gamma-1)} \right)} \quad (21)$$

We would like to highlight the density of the chamber differential with respect to the change in time. From this and the ideal gas relationship, we are able to isolate the change in combustion chamber pressure with respect to time. Let's walk through that now.

$$\begin{aligned} PV &= nRT \\ P &= \frac{n}{V} \cdot RT \\ P &= \rho RT \\ \rho &= \frac{P}{RT} \\ &\rightarrow \\ \frac{\partial \rho_{chmb}}{\partial t} &= \frac{1}{R' \cdot T_{chmb}} \cdot \frac{\partial P_{chmb}}{\partial t} \\ &\rightarrow \\ V_{chmb} \frac{\partial \rho_{chmb}}{\partial t} &= \frac{V_{chmb}}{R' \cdot T_{chmb}} \cdot \frac{\partial P_{chmb}}{\partial t} \end{aligned}$$

Substituting this in, we can then start the simplification and combination of liked terms to isolate the change in combustion pressure with respect to time.

$$\begin{aligned} A_b \cdot \rho_f \cdot \dot{r} + \dot{m}_{ox} &= A_b \cdot \rho_{chmb} \cdot \dot{r} + V_{chmb} \frac{\partial \rho_{chmb}}{\partial t} + P_{chmb} \cdot A_t \sqrt{\frac{\gamma}{R' T_{chmb}}} \left(\frac{2}{\gamma + 1} \right)^{\left(\frac{\gamma+1}{2(\gamma-1)} \right)} \\ \frac{V_{chmb}}{R' \cdot T_{chmb}} \cdot \frac{\partial P_{chmb}}{\partial t} &= A_b \cdot \rho_f \cdot \dot{r} - A_b \cdot \rho_{chmb} \cdot \dot{r} + \dot{m}_{ox} - P_{chmb} \cdot A_t \sqrt{\frac{\gamma}{R' T_{chmb}}} \left(\frac{2}{\gamma + 1} \right)^{\left(\frac{\gamma+1}{2(\gamma-1)} \right)} \\ \frac{V_{chmb}}{R' \cdot T_{chmb}} \cdot \frac{\partial P_{chmb}}{\partial t} &= A_b \dot{r} (\rho_f - \rho_{chmb}) + \dot{m}_{ox} - P_{chmb} \cdot A_t \sqrt{\frac{\gamma}{R' T_{chmb}}} \left(\frac{2}{\gamma + 1} \right)^{\left(\frac{\gamma+1}{2(\gamma-1)} \right)} \\ \frac{\partial P_{chmb}}{\partial t} &= \frac{R' \cdot T_{chmb}}{V_{chmb}} \cdot \left[A_b \dot{r} (\rho_f - \rho_{chmb}) + \dot{m}_{ox} - P_{chmb} \cdot A_t \sqrt{\frac{\gamma}{R' T_{chmb}}} \left(\frac{2}{\gamma + 1} \right)^{\left(\frac{\gamma+1}{2(\gamma-1)} \right)} \right] \end{aligned}$$

0.6.3 Appendix.C: Injector Flow Models

Exploration:

Compressible Fluid and Compressible Flow

Treating liquid nitrous oxide as an incompressible liquid is a fair and good assumption. However, this assumption breaks down for fluids for two cases: the velocity of the fluid or fluid body exceeds Mach 0.3 or the temperature of the fluid has increased. Both conditions change one intrinsic property, density. If the density of the liquid undergoes a change from the 5% reference point, that liquid can be considered compressible.

Thus when looking at the injector plate, is it reasonable to assume that across the plate the ΔP or change in pressures across it, is big enough to achieve this velocity? Or is it reasonable to assume that across the valving and injector plate, the change in temperature has increased so drastically that the density has changed?

With the analysis of the model set aside, let us look at the equations that will be used for the compressible flow model. One thing to note is that the effect of compressibility can be summed up into a coefficient as follows...

$$Y = \frac{\dot{m}_{compressible}}{\dot{m}_{incompressible}} \quad (22)$$

However, a specific equation developed by Zimmerman based on the research of the nonideal gas flow by Cornelius and Srinivas created an equation for the venturi flow of nitrous oxide. That is the equation below...

$$Y' = \sqrt{\frac{P_0}{2\Delta P} \left(\frac{2n}{n-2} \right) \left(1 - \frac{\Delta P}{P_0} \right)^{\frac{2}{n}} \left[1 - \left(\frac{\Delta P}{P_0} \right)^{\frac{n-1}{n}} \right]} \quad (23)$$

$$n = \gamma \left[\frac{Z + T \left(\frac{\partial T}{\partial Z} \right)_\rho}{Z + T \left(\frac{\partial T}{\partial Z} \right)_P} \right] \quad (24)$$

In most cases, P_0 which is the upstream stagnation pressure can oftentimes be assumed as the upstream pressure is well known and can be assumed to be the oxidizer tank pressure. The next is determining n or the isentropic power law exponent. The biggest issue is to accurately determine the necessary components to calculate this. A source suggests using REFPROP computer program by the National Institute of Standards and Technology (NIST). While the computer program is great, it is about \$350 for a license.

This begs the question, for the increased credibility of a little bit of the model, is a price tag this big worth it?

Last thing to consider if we were to move forward with this model is when this model is applicable. Generally, Zimmerman et al say that is the pressure differential across the injector (ΔP) is less than 50 psi the fluid can be considered incompressible. Since we are predicting more than 50 psi pressure drop, the fluid is incompressible.

Other Single Phase Flow Improvements

Other than the incompressible and compressible assumption, there are two other effects that can be considered due to the inlet geometry. These two effects are...

1. Vena Contracta Diameter Constriction Flow
2. Reynolds Number Skin Friction Viscous Flow

To summarize, these are more precise models that affect the discharge coefficient based on the Length and Diameter (L/D) ratio of the port holes drilled into the injector plate. Essentially, these are determinable by the inlet geometry and must be validated with a cold flow test. Furthermore, non-uniform inlet flow is a key assumption for these two later models. Of the three models above in the Single Phase Flow, they have been widely accepted and employed with great success and validation for Hybrid Rocket applications.

Two Phase Flow

Now that we know the flow will most likely be compressible, why do most research models bypass this? That is because the loss due to the liquid being incompressible is much less than the loss due to not modeling the second phase. The mass flow that exits the injector is not pure liquid anymore but a ratio of vaporous and liquid nitrous oxide. As the liquid accelerates through the drain port and into the injector, it expands leading to a drop in static pressure below the saturation pressure. This leads to the liquid nitrous oxide boiling off into the vaporous phase for a gaseous nitrous oxide.

This can be demonstrated by the following image. In the event that the bulk static pressure drops below the saturation temperature, a two-phase flow can occur leading to a reduced mass flow across the injector. This phenomenon is called **critical flow**, which describes a limit to the mass flow of oxidizer no matter how much you decrease the downstream pressure.

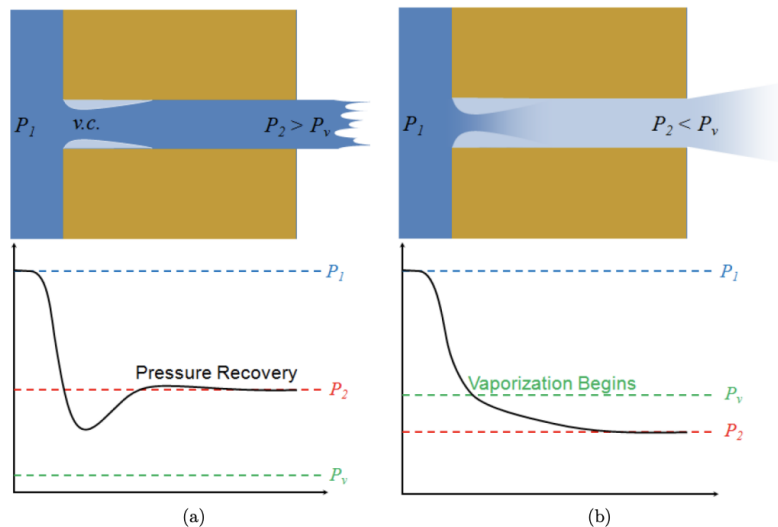


Figure 2.17: Conceptual injector pressure history as adapted from work by Dyer et al. showing (a) low vapor pressure propellant and (b) high vapor pressure propellant with flow from left to right [30]. The minimum area of contraction due to flow separation is denoted by v.c. (vena contracta).

To bring more complexity to the two-phase model, it can further be separated into equilibrium and non-equilibrium models. Each with its own subsets of models to determine the critical flow of the two-phase injector. These classifications are...

1. Equilibrium - models that assume a thermodynamic equilibrium between the liquid and gaseous phases throughout expansion
 - Homogeneous - The velocities of the liquid and vapor phases are equal
 - Non-homogeneous - a slip ratio k is defined such that there is an unequal velocity of liquid and vapor
2. Non-equilibrium - models that have generalized or fixed ratios of liquid and gaseous phases
 - Frozen - a slip ratio that is not equal but is fixed
 - Non-homogeneous - a slip ratio that is not equal

There are many models with extreme credibility and applications. However, I would like to put a pin in the exploration now before moving into more math. This will later be discussed in the conclusion.

Conclusion:

After researching and exploring the possible ways to improve the current standing oxidizer mass flow rate model and equations, it has become evident that the possible models out there may be too complex and require quite a bit of manpower only to have marginal improvements in accuracy.

Additionally, with the requirements for the CHIMERA hybrid rocket project, it really begs the question if Bernoulli's incompressible fluid first principle is good enough especially if the hybrid rocket burn time may be anywhere from 4 to 12 seconds.

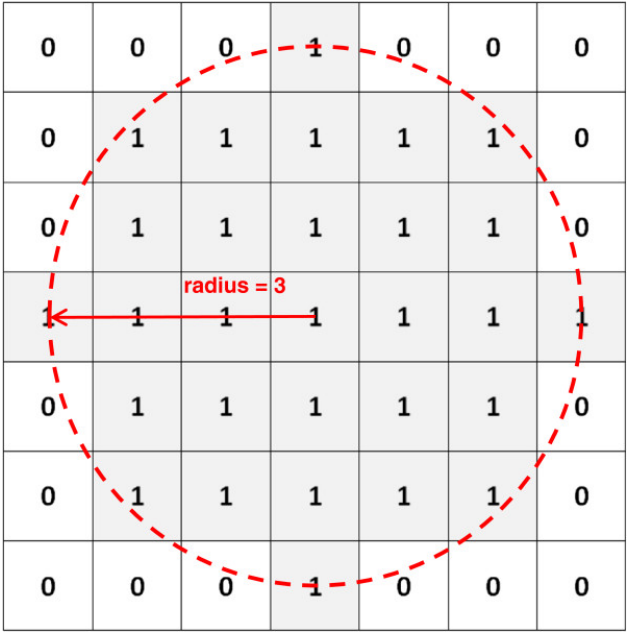
The first issue is determining the vapor fraction of nitrous oxide incoming to the injector before many of the models can be applied. Thus a blowdown model such as the ZK model, may be a more beneficial use of time. Lastly, from what I can tell, all of the models still require a cold flow test validation. Thus, it may save us time and manpower to do this after the cold flow or not at all as the initial Bernoulli's Compressible Flow is still an amazing model for our purposes.

0.6.4 Appendix.D: Derivations of Thrust and Exit Velocity

0.6.5 Appendix.E: Disk Filter

The majority of the coding comes from the implementation of the disk filter and contours.
apply_disk_filter()

This function calls the disk filter. It starts by creating a disk shaped kernel. The pixel img can be treated as a matrix, where each value in the matrix is either a 1 (255 or white) or 0 (black).



From this kernel, there is a additional mask that overlays it. This mask is circular and everything inside of it will be propellant gas or white pixels. The last call will apply this filter and mask combo onto the current state of the fuel grain geometry, applying the pixel blur. This is then passed into a separate threshold function to determine the fuel regression for the iteration.

0.7 Works Cited:

1. Arena, Zach, et al. Hybrid Rocket Motor California Polytechnic State University.
2. Fernandez, Margaret. "Propellant Tank Pressurization Modeling for a Hybrid Rocket." Theses, Jan. 2009, <https://scholarworks.rit.edu/theses/7111>.
3. Gieras, Marian, and Aleksander Gorgeri. "Numerical Modelling of the Hybrid Rocket Engine Performance." *Propulsion and Power Research*, vol. 10, no. 1, Mar. 2021, pp. 15–22. ScienceDirect, <https://doi.org/10.1016/j.jprr.2021.03.001>.
4. Kumar, Rajiv, and Ramakrishna Periyapatna. "Measurement of Regression Rate in Hybrid Rocket Using Combustion Chamber Pressure." *Acta Astronautica*, vol. 103, Oct. 2014, pp. 226–34. ResearchGate, <https://doi.org/10.1016/j.actaastro.2014.06.044>.
5. Numerical Modeling and Test Data Comparison of Propulsion Test Article Helium Pressurization System. <https://doi.org/10.2514/6.2000-3719>. Accessed 29 Sept. 2023.
6. Predoi, Ștefan, et al. "The Regression Rate-Based Preliminary Engineering Design of Hybrid Rocket Combustion System." *Processes*, vol. 10, no. 4, 4, Apr. 2022, p. 775. <https://doi.org/10.3390/pr10040775>.
7. Richard Nakka's Experimental Rocketry Site. <http://www.nakka-rocketry.net/index.html>. Accessed 10 Oct. 2023.
8. Sutton, George P., and Oscar Biblarz. *Rocket Propulsion Elements* (9th Edition).
9. Waxman, Benjamin S., "AN INVESTIGATION OF INJECTORS FOR USE WITH HIGH VAPOR PRESSURE PROPELLANTS WITH APPLICATIONS TO HYBRID ROCKETS". Stanford University, 2014.
10. Ziliac, Greg, and Mustafa Karabeyoglu. "Modeling of Propellant Tank Pressurization." 41st AIAA / ASME / SAE / ASEE Joint Propulsion Conference & Exhibit, American Institute of Aeronautics and Astronautics, 2005. DOI.org (Crossref), <https://doi.org/10.2514/6.2005-3549>.
11. Zimmerman, Jonah E., et al. "Review and Evaluation of Models for Self-Pressurizing Propellant Tank Dynamics." 49th AIAA/ASME/SAE/ASEE Joint Propulsion Conference, American Institute of Aeronautics and Astronautics, 2013. DOI.org (Crossref), <https://doi.org/10.2514/6.2013-4045>.